SEBHA UNIVERSITY CONFERENCE PROCEEDINGS, VOL.5 NO. 4 2026
DOI: 10.51984/JYBF9E28

وقائع مؤتمرات جامعة سبها
Sebha University Conference Proceedings
Conference Proceeding homepage: http://www.sebhau.edu.ly/journal/CAS

Processing and characterization of Libyan silica sand for welding, electrical, and solar technologies

N.A. Abdulgader[a], Hana Jamhour[b]*, Salem Alssaid[c], Maryam Morgham[b], Dareen Jummah Altarabulsi[d], Reema Ali Almuqouz[f], Ali Ben Ahmed[j]

[a] University of Algafara, Faculty of Science, Department of Physics, Algafara, Libya.
[b] Libyan Advanced Occupational Center for Welding Technologies, Tripoli, Libya.
[C] University of Sabha, Faculty of Information Technology, Sabha, Libya.
[d] Libyan Advanced Center for Chemical Analysis, Tripoli, Libya.
[f] Libyan Academy, Faculty of Science, Department of Physics, Tripoli, Libya.
[j] University of Sfax, Higher Institute of Biotechnology of Sfax, Sfax, Tunisia.

Keywords:
Silica sand
Silicon extraction
Quartz phase transition
XRD analysis
Thermal treatment
Purification
welding and Photovoltaic applications.

A B S T R A C T

High-purity silica is essential for advanced welding consumables, electrical insulation, and solar applications. This study focuses on improving the characteristics of natural silica sand from Adri Al-Shati, Libya, and assessing its industrial applicability to contribute to the systematic understanding of silica resources in the country. Ultra-fine milling and inorganic acids were used to achieve controlled chemical purification of raw silica to remove metallic impurities. The removal of these impurities enhances the dielectric characteristics of the material, which is an ideal precursor for photovoltaic (PV) technologies, electrical insulation, and welding. Silica sand (RA1), nano-milled silica powder (RA2), and purified (RA3) samples were characterized using X-ray fluorescence (XRF), X-ray diffraction (XRD), Fourier-transform infrared spectroscopy (FT-IR), and thermogravimetric analysis (TGA). RA3 was then heated at 1200, 1400, and 1600 °C. Sieve analysis demonstrated a well-defined particle size distribution suitable for the above applications. XRF showed that the SiO_2 purity increased from 91.7% to 99.36%, with a significant decrease in Fe_2O_3 from 0.103% to 0.082% and CaO from 4.12% to 0.478%. XRD and FTIR analyses revealed significant phase transformations from quartz to tridymite and cristobalite above 1200 °C. These high-temperature phase transformations are expected to influence the properties of welding slags, including viscosity and slag detachability. TGA and derivative thermogravimetric (DTG) results demonstrated excellent thermal stability and well-defined thermal decomposition behavior. Overall, this study provides a sustainable approach for the production of high-purity silica from locally available resources, which fulfills stringent technical requirements for advanced industrial applications. The results show the possibility of the use of local raw materials as an economical alternative for the support of industrial self-sufficiency and future use in metallurgical and high-tech areas.

معالجة وتوصيف رمال السيليكا الليبية لتقنيات اللحام والكهرباء والطاقة الشمسية

نصرعبد القادر الجطيلاوي [أ]،هناء جمهور [ب]*،سالم الصيد [ج] ، مريم مرغم[ب]، دارين جمعة محمد الطرابلسي[د]،ريمة المقوس[و]، علي بن أحمد [ر]

[أ] جامعة الجفارة ، كلية العلوم ، قسم الفيزياء ،الجفارة، ليبيا
[ب] المركز الليبي المهني المتقدم لتقنيات اللحام ، طرابلس، ليبيا
[ج] جامعة سبها ، كلية تقنية المعلومات،جامعة سبها، ليبيا
[د] المركز الليبي الليبي المتقدم للتحاليل الكميائية، طرابلس، ليبيا
[و] الأكادمية الليبية، قسم الفيزياء ، طرابلس، ليبيا
[ر] جامعة صفاقس ، المعهد العالي للبيوتكنولوجيا بصفاقس، صفاقس، تونس

*Corresponding author: Hana Jamhour
E-mail addresses: amnagred@gmail.com ,(N.A. Abdulgader)nabdulgader7@hotmail.com ,(S. Alssaid)sal.alsaid@sebhau.edu.ly ,(M. Morgham)mariammorgham@gmail.com ,(D. J. Altarabulsi)Dareengiuma@gmail.com ,(R. A. Almuqouz)Reemallmagooz@gmail.com ,(A. Ben Ahmed)ali.benahmed@isbs.usf.tn

Article History : Received 30 May 2026 - Received in revised form 30 September 2026 - Accepted 11 November 2026

الملخص

تعتبر السيليكا عالية النقاء ضرورية لمواد اللحام المتقدمة والعزل الكهربائي وتطبيقات الطاقة الشمسية. تركز هذه الدراسة على تحسين خصائص رمل السيليكا الطبيعي من أدري الشاطئ، ليبيا، وتقييم قابلية التطبيق الصناعي للمساهمة في الفهم المنهجي لموارد السيليكا في البلاد. استُخدم الطحن فائق الدقة وطريقة التنقية الكيميائية لتحقيق نقاوة للسيليكا الخام ولإزالة الشوائب المعدنية. حيث تُحسّن إزالة هذه الشوائب الخصائص العازلة للمادة، والتي تعد مقدمة مثالية لتقنيات الطاقة الكهروضوئية (PV) والعزل الكهربائي وكذلك لتقنيات اللحام. تم توصيف عينات رمل السيليكا (RA1)، ومسحوق السيليكا المطحون النانوي (RA2)، والسليكا المنقاة (RA3) باستخدام الأشعة السينية الفلورنسية (XRF)، حيود الأشعة السينية (XRD)، التحليل الطيفي للأشعة تحت الحمراء لتحويل فوريه (FT-IR)، وتحليل قياس الوزن الحراري (TGA). ثم سخنت (RA3) الى درجات حرارة مختلفة 1200,1400و 1600 درجة مئوية. وأظهرت نتائج تحليل المنخل توزيعًا دقيقًا لحجم الجسيمات، مما يجعله مناسبًا للتطبيقات المذكورة. كما كشف تحليل الأشعة السينية الفلورية (XRF) عن زيادة في نقاء ثاني أكسيد السيليكون (SiO_2) من 91.7% إلى 99.36%، مع انخفاض ملحوظ في أكسيد الحديد الثلاثي (Fe_2O_3) من 0.103% إلى 0.082%، وأكسيد الكالسيوم (CaO) من 4.12% إلى 0.478%. وأظهرت تحليلات حيود الأشعة السينية (XRD) وتحليلات الأشعة تحت الحمراء بتحويل فوريه (FTIR) تحولات طورية كبيرة من الكوارتز إلى الترايديميت والكريستوباليت عند درجات حرارة أعلى من 1200 درجة مئوية. ومن المتوقع أن تؤثر هذه التحولات الطورية عند درجات الحرارة العالية على خصائص خبث اللحام، بما في ذلك اللزوجة وسهولة فصل الخبث. حيث أظهرت تحليلات التحليل الحراري الوزني (TGA) والتحليل الحراري الوزني التفاضلي (DTG) استقرارًا حراريًا ممتازًا وسلوكًا واضحًا للتحلل الحراري. وبشكل عام، تقدم هذه الدراسة نهجًا مستدامًا لإنتاج السيليكا عالية النقاء من موارد محلية متوفرة، وهو ما يفي بالمتطلبات التقنية الصارمة للتطبيقات الصناعية المتقدمة. وتُظهر النتائج إمكانية استخدام المواد الخام المحلية كبديل اقتصادي لدعم الاكتفاء الذاتي الصناعي، فضلًا عن استخدامها مستقبلًا في مجالات التعدين والتكنولوجيا المتقدمة.

الكلمات المفتاحية:

رمل السيليكا
استخلاص السيليكون
تحول طور الكوارتز
تحليل حيود الأشعة السينية
المعالجة الحرارية
التنقية
تطبيقات الخلايا الكهروضوئية.

1. Introduction

Silica is one of the most abundant compounds in the Earth's crust, constituting approximately 59% of its total composition. It exists in various crystalline and amorphous forms, with quartz being the most thermodynamically stable polymorph under ambient conditions [1-4]. The unique physicochemical properties of silica, including high thermal stability, chemical inertness, excellent dielectric strength, and a wide bandgap (~9 eV), render it indispensable for numerous advanced technological applications, ranging from microelectronics and photovoltaics to high-temperature metallurgy [5-6]. In recent years, increasing attention has been directed toward the sustainable utilization of naturally occurring silica resources as strategic raw materials for high-value industrial applications. The growing demand for environmentally sustainable and locally available mineral resources has encouraged extensive research on the purification and functional modification of silica sands for advanced engineering applications, particularly in welding consumables, electrical insulation, and photovoltaic materials. Consequently, the development of efficient purification strategies capable of producing high-purity silica from indigenous resources has become an important research priority. Specifically, in fusion welding and joining processes, silica serves as a crucial acidic constituent in flux formulations, where its high temperature phase stability and slag forming characteristics are vital for shielding molten metal and stabilizing arcs [7-8]. In recent decades, the global demand for high purity silica has escalated dramatically, driven by the strict quality benchmarks required in modern welding consumable manufacturing, semiconductor electronics, and photovoltaic (PV) solar cells [6]. In advanced arc welding processes, such as Submerged Arc Welding (SAW), the chemical purity, particle morphology, and crystalline phase of silica directly influence the viscosity, oxygen potential, and thermodynamic behavior of the welding slag [9]. Under ambient conditions α - quartz is the stable polymorph, crystallizing in the trigonal system with lattice parameters of a = 4.913 Å and C = 5.405 Å [7, 10]. Upon thermal exposure, silica undergoes a sequence of displacive and reconstructive phase transformations:

$$\alpha - Quartz \xrightarrow{\approx 573} \beta - Quartz \xrightarrow{\approx 850} \beta - Tridymite \xrightarrow{\approx 1470} \beta - Cristobalite \xrightarrow{\approx 1713} Melt$$

In high-temperature metallurgy and advanced fusion welding, the kinetics of these phase transitions, particularly the transformation into cristobalite is highly critical. Cristobalite features a diamond-like cubic structure that provides high thermal stability and a low coefficient of thermal expansion, making it a vital component in refractory matrices and slag-forming systems [7], [11]. However, in natural silica sands, the presence of localized mineral impurities acts mineralizing agents, altering the activation energy and lowering these theoretical transformation temperatures [12,13]. Commercially available natural silica sands typically contain 70–99% SiO2, while the remaining fraction consists of detrimental impurities such as Al2O3 (0.1–5.0 wt.%), Fe2O3 (0.01–1.0 wt.%), TiO2 (0.01–0.5 wt.%), and various alkali/alkaline earth oxides (CaO, MgO, Na2O, K2O) [7]. For specialized engineering applications, these impurities must be strictly reduced to parts-per-million (ppm) levels [14]. In advanced arc welding consumables, such as Submerged Arc Welding (SAW) fluxes and flux-cored wires, the chemical purity of SiO2 directly governs the viscosity, oxygen potential, and electrical conductivity of the molten slag [15]. Excessive impurities (e.g., phosphorus, sulphur, or unstable oxides) promote element transfer into the weld pool, leading to severe defects such as hot cracking and degraded fracture toughness in high-strength steel joints [8]. Similarly, for electronic-grade insulating materials and photovoltaic (PV) solar-grade silicon production, a high-purity precursor is mandatory to prevent carrier trapping and ensure optimal dielectric strength [3,16]. Consequently, this multisectoral demand has intensified the search for high-purity raw silica sources that are highly amenable to precise purification, thermal modification, and nanostructuring. Libya possesses substantial natural mineral wealth, including vast deposits of high-quality silica sands distributed across its desert regions. The southwestern territory, particularly the Wadi al-Shati and Murzuq

basins, is recognized for its extensive sand formations characterized by high silicon dioxide content and low baseline impurity levels [14,17,18]; Research aimed at purifying and physically tailoring these local resources for advanced industrial applications has historically been limited. Previous studies, including those by Zreiba and Dweiby [19], Rahuma et al. [20], and El-Taher et al. [21], have established the mineralogical and elemental suitability of Libyan silica sands and their potential for industrial applications. However, a critical research gap remains regarding the advanced processing, phase transformation behaviour, and nano-powder synthesis of these indigenous sands to meet the stringent requirements of high-tech industries. Although previous investigations have confirmed the suitability of Libyan silica sands for conventional glass manufacturing and ceramic applications, comprehensive studies integrating chemical purification, particle-size optimization, thermal stability, phase transformation, and structural characterization for advanced submerged arc welding (SAW), electrical insulation, and photovoltaic applications remain scarce. Therefore, further systematic investigations are required to establish the scientific basis for utilizing Libyan silica sands as high-value engineering materials for advanced technological applications. To address this research gap, the present study proposes a comprehensive physicochemical processing route for Libyan silica sand obtained from the Adri Al-Shati region. The investigation includes controlled chemical purification, particle-size optimization, and multi-technique characterization using XRF, XRD, FTIR, TGA/DTA, and SEM analyses. In addition, the phase evolution of purified silica following thermal treatment at 1200, 1400, and 1600 °C is systematically evaluated to determine its potential as a precursor material for advanced submerged arc welding (SAW) fluxes, electrical insulation, and photovoltaic technologies. This research encompasses the complete processing chain, starting from raw material beneficiation and chemical purification to advanced nano-powder synthesis. Since welding, electrical insulation under stress, and photovoltaic silicon processing are inherently high-temperature phenomena, the synthesized nano-powders were subjected to sustained thermal treatments at 1200, 1400 and 1600 ºC for a duration of 3 hours. The resulting structural, chemical, and thermal evolutions were thoroughly evaluated through a comprehensive suite of characterization techniques. This includes X-ray Diffraction (XRD) to track crystalline phase transformations, X-ray Fluorescence (XRF) to verify elemental purity [22], and Fourier-Transform Infrared Spectroscopy (FTIR) to monitor structural bonding variations [23]. Furthermore, Thermogravimetric analysis (TGA) coupled with derivative thermogravimetric analysis (DTG) were performed from 25 to 800 °C at a heating rate 10 °C min^{-1} to evaluate the thermal stability, moisture removal, volatile loss, and phase-transition behavior of the purified silica [24].

2. Experimental work

This section explains the experimental methods used to prepare and analysed SiO_2 nano powder from a local sand in Libya.

2.1. Material

The Source of SiO_2 in this study was taken from the crust Sand, specifically the Adari silica sand, which was of good quality and found in the southwestern Libyan region, in the Wadi al-Shati area, 700 km from the capital, Tripoli. This region is known for its desert nature and contains high-quality pure sands, as shown in the geographical location of the area in Figure 1

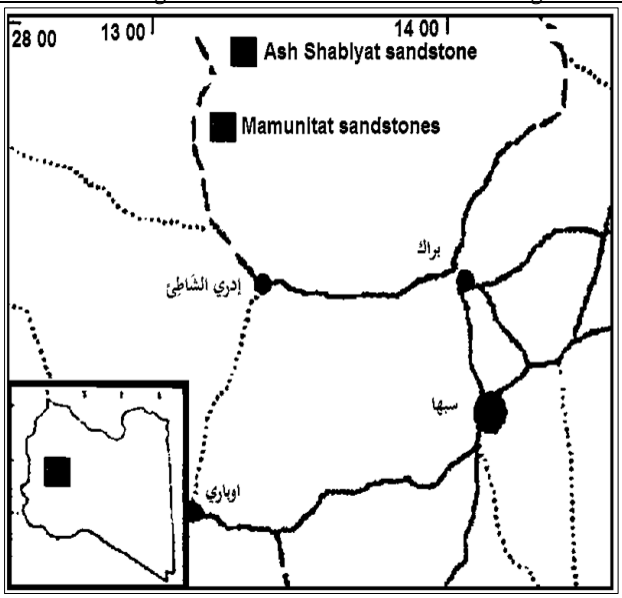


Fig. 1: Location of Source SiO_2 **[24-25]**

2.2. Chemical material and lab tools

Every Material and lab tool utilized in the experimental for designation of Sand and characteristics of silica nanopowder was listed in Table 1.

Table 1: Material and lab tools

Chemical Material and lab tools	Manufacturer/type
Hydrochloric Acid	35-38% Eurostar Scientific/uk
Nitric Acid	96% Eurostar Scientific/uk
Sulfuric Acid	97% Eurostar Scientific/uk
HF	50% Eurostar Scientific/uk
Electronic weight balance	Sartorius,1000 ± 0.0001g
Dry pressing	Specac/Italy
Glass ware	Commercial

The sample was cleaned and dried at 100 °C degrees in a furnace for a period of 24 hours to eliminate contamination from the sand. Following that, 2000 g of sand were split using a John Riffle splitter until 200 g were obtained as a representative specimen. The representative specimen was then sieved within 25 min through a series of sieve sizes: 425, 212, 150, 106, 75, and 45 µm, as shown in Figure 2. After the process is complete, weigh each retained material to find the average particle size by calculating the cumulative passing and retained material represented by a plot chart, where evaluating the sample's particle size is essential for producing nano powder.



Fig. 2: Sieving analysis

2.3. Production of nano powder

The obtained Sample was sieved to give particles of less than 75µm in size, which was subjected to a high energy centrifugal ball milling machine (Retsch GmbH, S100) to produce a nano powder. The centrifugal milling was done at 600 rpm for 2 hours. The phase and chemical composition of the obtained nano powder were analyzed via XRD, XRF, FT-IR, and TGA.

2.4. Purification of nano-powder silica by digestion and precipitation process

The samples underwent preliminary purification through chemical treatment using a combination of inorganic acids (HCl, H_2SO_4, HNO_3, HF) and distilled water. This step aimed to remove mineral impurities and reduce the proportions of undesirable elements that negatively affect the purity of the silica. A detailed description of the steps can be explained by the processes in Figure 3 below.

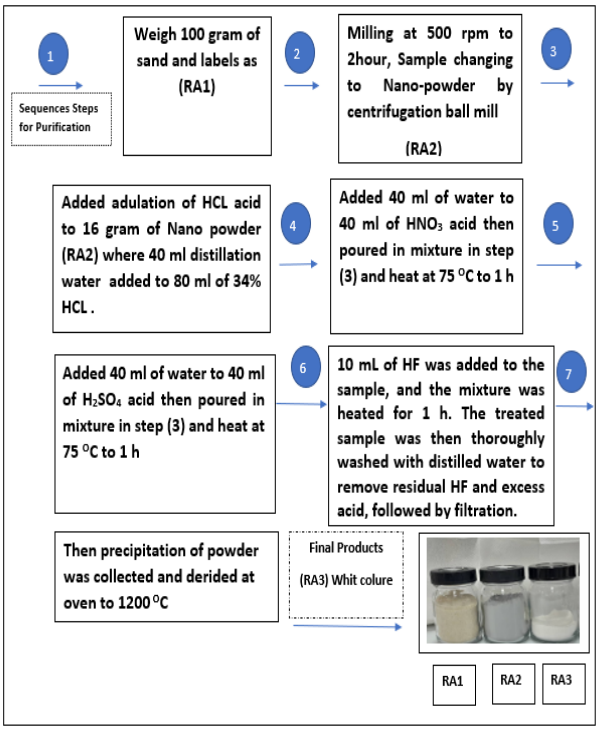


Fig. 3: Sand purification process

After adding the acids shown in the chemical treatment diagram, the filtration process takes place to obtain a pure precipitate and the sample is washed with distilled water to remove any remaining impurities as shown in the figure (4). Then heated the samples to 1000 °C for giving crystalline powder and removal of any water in the structural.

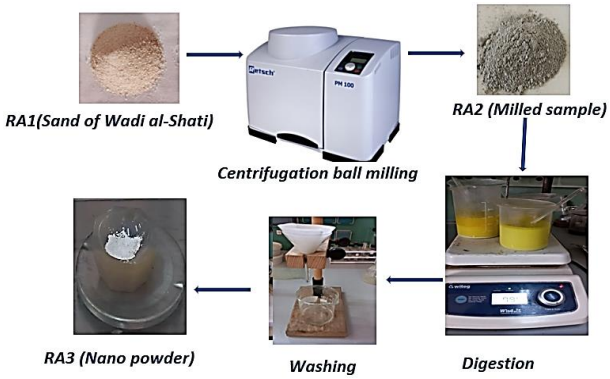


Fig. 4: Digestion and precipitation process

2.5. Characterization

To identify the phase composition and content of the samples, the silica sand, nano-milled silica powder, and purified silica powder (obtained via the digestion and precipitation process) were characterized using different analytical techniques, including XRD, XRF, TGA, and FT-IR. X-ray diffraction (XRD) analysis was performed to identify the crystalline phases and evaluate the structural characteristics of the silica sand obtained from Adri Al-Shati, Southern Libya. The measurements were conducted using a computerized Philips PW 1800 X-ray diffractometer (Philips N.V., The Netherlands) with Cu-Kα radiation (λ = 1.5406 Å) and were carried out at the Libyan Petroleum Institute, Tripoli, Libya. Three sample conditions were investigated: the raw silica sand (RA1), the milled powder (RA2), and the purified silica powder (RA3). The diffraction patterns were recorded over the selected 2θ range using a step time of 1 s, a tube voltage of 40 kV, and a tube current of 30 mA. The obtained XRD patterns were presented as diffraction intensity (I) as a function of the diffraction angle (2θ). The crystalline phases present in the RA1, RA2, and RA3 samples were identified by comparing the observed diffraction peaks with standard reference data. The average crystallite size of the RA2 and RA3 powders was estimated from the broadening of the major diffraction peaks using the Scherrer equation:

$$D = K\lambda / (\beta \cos \theta) \quad \ldots\ldots\ldots\ldots\ldots\ldots\ldots\ldots\ldots\ldots\ldots\ldots (1)$$

where D is the mean crystallite size, K is the dimensionless shape factor (typically taken as approximately 0.9), λ is the wavelength of the incident X-ray radiation (1.5406 Å for Cu-Kα radiation), β is the full width at half maximum (FWHM) of the diffraction peak expressed in radians after correction for instrumental broadening, and θ is the Bragg diffraction angle. It should be noted that the crystallite size calculated using the Scherrer equation represents the mean size of coherently diffracting crystalline domains and may be smaller than, or equal to, the actual grain size. The calculated crystallite-size values for the RA2 and RA3 samples are presented in Table 6. The chemical composition of the samples, silica sand (RA1), milled Sand (Nano-powder RA2) and purified silica (RA3) was determined by XRF analysis; the XRF analysis was performed using the portable Spectro x SORT XHHO3 equipment. The Tensor II spectrometer from Bruker was used for FTIR testing to investigate the chemical groups in the samples, and the analysis was carried out at the Libyan Polymer Research Center. The GOLLEMBR Solution (TGA BAXT-TGA101) equipment was used to perform Thermal Gravimetric Analysis (TGA) on Samples. The analysis was carried out in a nitrogen environment between 25 and 800 °C, with a heating rate increment of 20 °C/min. The TGA results' normal and derivative curves were acquired for the Samples.

2.6. Prepared sample via dry pressing

The purification powder (RA3) was pressed to make disc with 1cm diameter at pressure 10 pa for a holding time about 10 min, The samples were pressed after chemical treatment inside the Libyan polymer Research Center; Tripoli- Libya with a weight of 1.33g and the addition of drops of acetone for the purpose of softening the sample and making it more cohesive inside the pressing device as shown in Figure (5) to be heated at different range of temperature (1200,1400, 1600 °C) (RT1, RT2, RT3).



Fig. 5: Pressing samples

3. Results and Discussion

3.1. Sieve analysis

The sieve analysis results in Table 2 and Figure 6 revealed that the raw silica sand exhibits a relatively uniform particle size distribution. The highest fraction of the sample, 47.42 wt.%, was retained on the 50 mesh (300 µm), followed by 30.90 wt.% retained on the 70 mesh (212 µm). These two fractions together account for approximately 78.32 wt.% of the total sample, indicating that the silica sand is predominantly composed of particles within the 212-300 µm size range. The percentages retained on the finer sieves 80-200 mesh gradually decreased, demonstrating a continuous and well-graded particle size distribution. This relatively uniform granulometric distribution provides a suitable feedstock for subsequent milling, facilitating efficient particle size reduction and the production of

homogeneous Nano silica powder. The effectiveness of this approach was confirmed by the subsequent XRF and XRD analyses, which demonstrated a high SiO_2 purity (99.36 wt.%) and the preservation of the crystalline quartz phase. Therefore, the initial particle size distribution played a key role in producing high-quality Nano-silica suitable for advanced applications in welding materials, electronic devices, and photovoltaic technologies. Similar results have been reported by other researchers [25-26].

Table 2: Sieve analysis

Sieve Weight (gm)	Aperture size (Mesh)	%Retained Weight
19.88	Log10 (50) =1.7	47.42%
12.77	Log10 (70) =1.85	30.9 %
4.68	Log10 (80) =1.9	11.1 %
0.83	Log10 (120) =2.07	1.97 %
3.55	Log10 (140) =2.15	8.46 %
0.14	Log10 (170) =2.23	0.33 %
0.078	Log10 (200) =2.3	0.18 %
Total Weight (gm)	**Weight (gm)**	**Loss Weight (gm)**
37.84	37.61	0.19

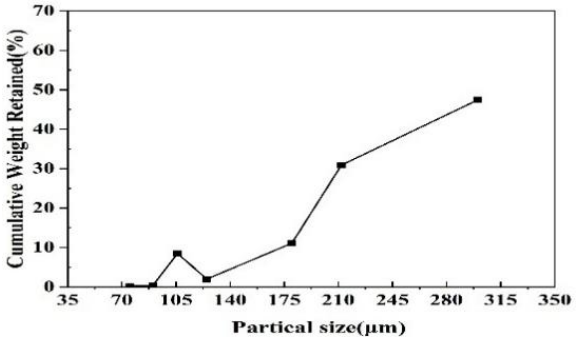


Fig. 6: Cumulative Weight retained (%).vs, particle size (µm) for Adari silica sand.

3.2. Results of XRD analysis

To determine the phase composition, lattice parameters, and grain size of samples, X-ray diffraction spectra were obtained before and after chemical treatment (RA1) and (RA3). These results were compared to a standard sample (NR5) and aligned with findings from previous studies [26][27], [28], and [29], confirming that the material crystallize in the hexagonal system as calculated through the appropriate lattice constant formula.

$$\frac{1}{d^2{}_{hkl}} = \frac{4}{3}\left(\frac{h^2 + hk + k^2}{a^2}\right) + \frac{l^2}{c^2} \qquad (2)$$

Shown in Tables (3-5), where (d) is the perpendicular distance between the adjacent planes, the Miller indices (hkl) identify the crystallographic planes, whereas the lattice parameters (a and c) and their axial ratio (c/a) characterize the crystal structure of the quartz phase in the silica sample. The analysis of Sands before and after chemical treatment through X-ray diffraction (XRD) shows that the samples are largely consistent with the standard sample (NR5). The pre-treatment samples contained impurities, particularly high Free silicon dioxide, with distinct crystalline peaks noted at (2θ = 26º). Post-treatment results indicate less impurity and a predominant presence of pure α-quartz, with a decrease in peak intensity at various angles. The lattice constants were calculated using the Debye-Scherer equation and confirmed to be a = 4.9135 Å and c = 5.4051 Å, consistent with prior studies. Overall, the treated sands exhibit a significant reduction in peak intensity variation and peak broadening, indicating changes in crystallite grain size Table 6 and an increase in silica content, from approximately 91.7% to 99.36%, aligning with previous research findings regarding the crystalline structure and purity of the material Figures 7 and 8 [27-30].

Table 3: Miller indies for reference (NR5).

2Θ	COS2Θ	d (Å)	hkl	a (Å)	c (Å)
20.754	0.968	4.23607	100	4.89139	-
26.874	0.946	3.31480	101	-	.307945
35.474	0.823	2.44864	110	.897284	-
38.075	0.799	2.27507	102	-	.389965
40.724	0.773	2.012094	200	.89814	-
54.972	0.619	1.53991	211	-	5.49694
58.033	0.585	1.45120	113	-	5.40308
59.324	0.57	1.41623	300	.905964	-
60.706	0.555	1.38003	212	-	5.41399
.09461	0.55	1.36994	301	-	5.48841
64.569	0.511	1.28667	104	-	5.40085
66.019	0.495	1.25464	302	-	.430615
67.298	0.48	0.227731	220	4.91092	-
a3		c/a		C	a
112.66438		1.10524		5.41647	4.90073

Table 4: Lattice parameter for (RA1)

2Θ	COS²Θ	d (Å)	hkl	a (Å)	c (Å)
21.533860	6.965	4.12675	100	4.76554	-
27.09555	0.945	3.29100	101	-	5.614965
43.02499	0.865	2.10234	200	4.85517	-
50.75523	0.816	1.79881	112	-	5.60750
55.71617	0.7816	1.65256	103	-	5.42716
64.69191	0.713	1.43973	113	-	5.4717
68.80473	0.680	1.36031	212	-	5.86866
74.0502	0.637	1.27922	104	-	5.39119
78.90594	0.596	1.2869	220	4.45002	-
a3		c/a		C	a
103.174		1.18620		4.69019	5.56352

Table 5: Lattice parameter for purification sample (RA3)

2Θ	COS²Θ	d (Å)	hkl	a (Å)	c (Å)
72.06	0.94	3.29464	101	-	5.2704
36.957	0.89	2.43235	110	4.86414	-
40.70	0.87	2.21663	111	-	5.33433
42.87	0.865	2.10940	200	4.87139	-
50.53	**0.817**	**1.96535**	**201**	**-**	**5.4879**
50.700	**0.816**	**1.80354**	**003**	**-**	**5.4106**
55.71	**0.781**	**1.64845**	**103**	**-**	**5.37214**
66.23	**0.701**	**1.40997**	**300**	**4.8845**	**-**
68.53	**0.682**	**1.36809**	**301**	**-**	**5.8597**
a^3		**c/a**		**C**	**a**
115.739		**1.11952**		**4.87334**	**5.45584**

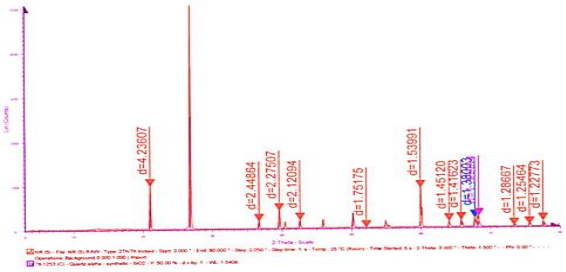


Fig. 7: X-ray spectrum of SiO_2 standard sample

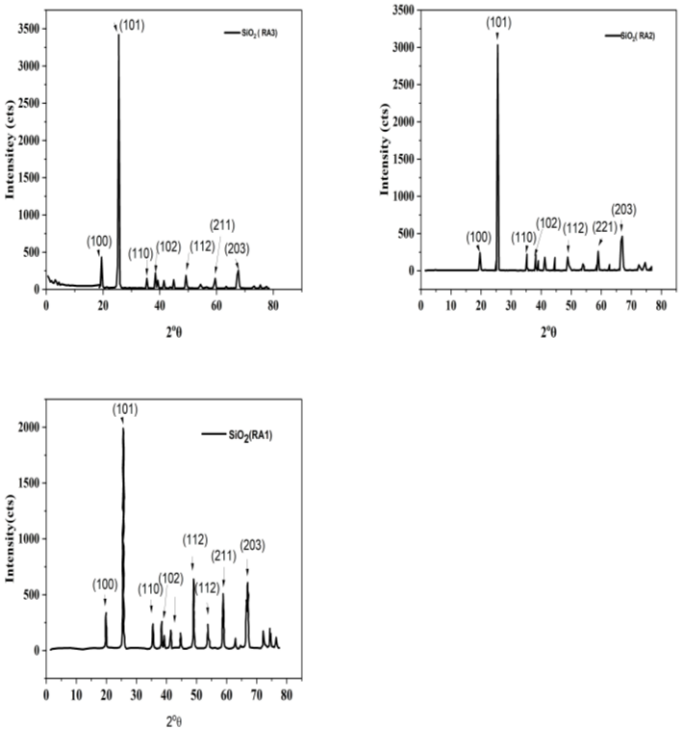


Fig.8: The peaks of the XRD spectrum of samples (R1, R2, and R3).

Table6: Grain size for nano-powder (RA2) and Purification (RA3)

Sample	θ (deg)	β (rad)	cosθ	D(nm)
RA2	54	0.00272	0.66	75.7
RA3	50	0.00394	0.625	66.17

Figure 9. XRD patterns of the purified SiO_2 powder after heat treatment at RT1 (1200 °C), RT2 (1400 °C), and RT3 (1600 °C), showing the persistence of the characteristic quartz diffraction peaks and retention of the principal crystalline SiO_2 phase after high-temperature treatment, reveal that the characteristic crystalline structure of SiO_2, especially the quartz (101) reflection at $2\theta = 26.6°$, is maintained. Although there were variations in peak intensity with temperature, the primary crystalline phase was recognizable even at 1600 °C, indicating thermal stability of the purified silica. This resilience is important for potential applications in high-temperature settings, such as welding, where silica is a key component in flux systems. Similarly, its high purity is advantageous for electrical and electronic uses, and for photovoltaic applications. However, while the findings validate the silica's thermal retention, further specific functional tests are needed for application suitability.

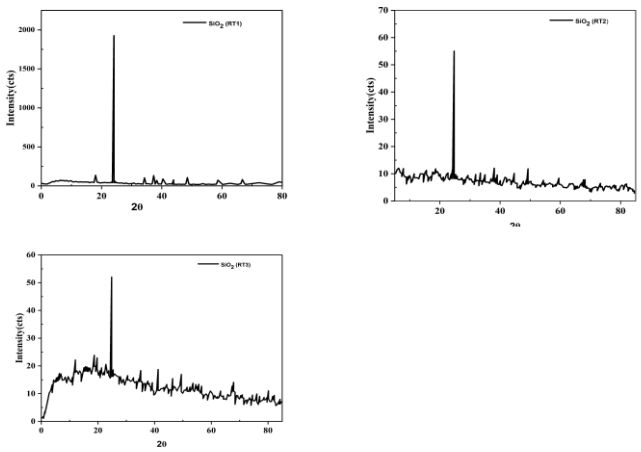


Fig.9: The peaks of the XRD of RA3 after heat treatment RT1(1200 ^{O}C), RT2(1400 ^{O}C) and RT3 (1600 ^{O}C).

3.3. XRF Results

The XRF results demonstrated that the purification process significantly enhanced the chemical purity of the Libyan silica sand. The SiO_2 content increased from 91.70 wt.% in the raw sample (RA1) to 99.361 wt.% after purification (RA3), accompanied by a substantial reduction in the concentrations of impurity oxides, particularly CaO and Fe_2O_3. The marked decrease in these impurity oxides is consistent with the removal of carbonate- and iron-bearing components during the purification process, resulting in a highly purified silica material suitable for high-value industrial applications. In addition to the improvement in chemical purity, the purification process resulted in only a limited reduction in sample mass. The mass of the milled silica powder decreased from 16.00 g (RA2) to 15.66 g after purification (RA3), corresponding to a mass recovery of 97.88% and a mass loss of approximately 2.13%. This relatively low mass loss may be attributed primarily to the removal of soluble and acid-reactive mineral impurities, together with minor material losses during washing, filtration, drying, and sample handling. A limited contribution from SiO_2 dissolution during the HF treatment cannot be completely excluded. Nevertheless, the high mass recovery suggests that substantial loss of the silica-rich fraction did not occur during purification. The measured SiO_2 purity of 99.361 wt.% is relevant to applications in which low concentrations of iron and other coloring impurities are desirable. The pronounced reduction in Fe_2O_3 is especially important for solar-energy applications because iron-bearing impurities can increase optical absorption and reduce the light transmittance of silica-based glass. Therefore, the purified silica may warrant further evaluation as a potential raw material for low-iron and photovoltaic glass applications. Although high optical transparency is important in these applications, optical and photovoltaic performance was not evaluated in the present study [25]. In welding technology, the chemical purity of silica is also an important consideration because SiO_2 can act as a major slag-forming component in selected welding flux systems. The substantial reduction in impurity oxides provides a more chemically controlled silica source that could be evaluated in appropriately formulated welding-flux systems when incorporated into appropriately formulated flux compositions. In particular, the reduced concentrations of CaO and Fe_2O_3 may influence slag chemistry and viscosity; this effect must be assessed using the complete flux formulation and welding parameters. However, the effects on arc stability, gas porosity, penetration, and cracking depend on the complete flux formulation and welding parameters and should therefore be verified through dedicated welding-performance tests [28]. Thus, the present XRF results support further investigation of the purified silica as a component of silica-containing welding fluxes. Furthermore, the improved chemical purity of the treated silica also justifies further evaluation for ceramic and electrical-insulation applications. The high SiO_2 content and reduced concentration of ionic and transition-metal impurities may be associated with favorable material characteristics; however, thermal, dielectric, chemical-resistance, and mechanical tests are required to verify these properties. These properties make the purified silica a promising candidate for high-temperature ceramic components, refractory formulations, and selected electrical-insulation applications, subject to further evaluation of the relevant thermal, dielectric, and mechanical properties.

Table 7: The comparison of Chemical composition of the Sand silica and purified silica powder determined by XRF analysis.

Oxide / Element	Formula	Raw silica (RA1) (wt.%)	Purified silica (RA3) (wt.%)
Silicon oxide	SiO_2	91.700	99.361
Aluminum oxide	Al_2O_3	3.540	—
Calcium oxide	CaO	4.120	0.478
Iron oxide	Fe_2O_3	0.103	0.082
Potassium oxide	K_2O	ND	0.034

Magnesium oxide	MgO	ND	—
Titanium oxide	TiO_2	0.330	—
Sulfur oxide	SO_3	0.210	—
Chloride	Cl	0.001	—
Zirconium oxide	ZrO_2	—	0.007
Silver	Ag	—	0.005
Cerium oxide	CeO_2	—	0.004
Lanthanum	La	—	0.003
Praseodymium	Pr	—	0.002
Nickel oxide	NiO	—	0.001
Zinc oxide	ZnO	—	0.001
Strontium oxide	SrO	—	0.001
Thorium	Th	—	0.001

3.4. Results of the thermal weight analysis

Figure 10 presents the thermogravimetric analysis (TGA) curves of silica sand collected from the Adari Al-Shati region at different processing stages, including the raw sand (RA1), finely milled sand (RA2), acid-treated sand (RA3), and the heat-treated samples at 1200 °C (RT1), 1400 °C (RT2), and 1600 °C (RT3). Approximately 2 mg of each sample was heated from room temperature to 600 °C under a nitrogen atmosphere at a heating rate of 20 °C min^{-1}. The untreated samples (RA1–RA3) exhibited greater mass losses than the heat-treated samples over the investigated temperature range. The initial mass loss below approximately 100 °C may be attributed primarily to the evaporation of physically adsorbed moisture, while the subsequent mass changes may be associated with surface hydroxyl groups, residual volatile species, and thermally unstable minor components present in the untreated silica. Among the untreated samples, RA3 exhibited the highest mass loss, reaching approximately 7.4% at 600 °C, whereas RA2 showed comparatively greater thermal stability. These differences indicate that the processing history and surface characteristics of the silica significantly affect its thermal response. In contrast, the heat-treated samples (RT1, RT2, and RT3) exhibited substantially improved thermal stability, with only limited mass loss throughout the investigated temperature range. RT3 retained approximately 98% of its initial mass at 600 °C, corresponding to a mass loss of approximately 2% under the stated conditions. The similar TGA profiles suggest that most readily volatilized or thermally unstable constituents had been removed before or during the preceding treatments. Any slight improvement observed with increasing treatment temperature may reflect further reduction of volatile or hydroxyl-containing species and increased structural stability. The thermal stability observed after high-temperature treatment is consistent with the XRF results, which demonstrated the high SiO_2 purity of the processed material, and with the XRD results, which confirmed the preservation and evolution of the crystalline silica structure following thermal treatment. The lower mass loss of the RT samples indicates greater mass stability under the investigated TGA conditions. From an application perspective, this improved thermal stability is relevant to the potential use of the purified silica in high-temperature materials, including welding flux formulations, refractory-related systems, electrical insulating materials, and photovoltaic-related silica precursors. However, the present TGA results demonstrate thermal stability rather than direct welding performance; therefore, the effects of the processed silica on slag behavior, arc stability, and weld quality require further experimental validation using actual welding trials [25-29].

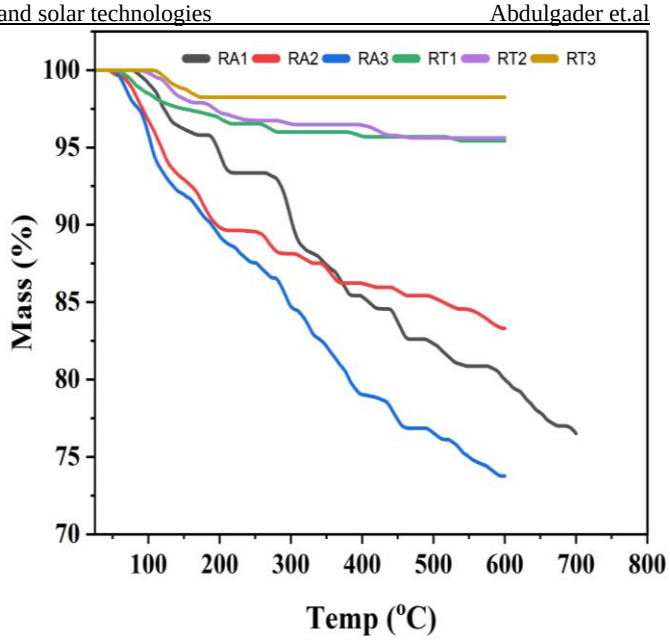


Fig.10: Thermal weight analysis of Nano -Silica after heat treatment process

3.5. Results of differential thermal analysis (DTA)

Figure 11 presents the derivative thermogravimetric (DTG) curves of silica sand samples from the Adri Al-Shati region at different processing stages, including the raw sand (RA1), finely milled sand (RA2), acid-treated sand (RA3), and the heat-treated samples at 1200 °C (RT1), 1400 °C (RT2), and 1600 °C (RT3). The DTG profiles show a reduction in the number and intensity of thermal events after processing of the silica throughout the purification process. The raw sand (RA1) exhibits numerous sharp DTG peaks over the investigated temperature range, reflecting successive thermal events associated with the desorption of physically adsorbed water, dihydroxylation of surface silanol (Si–OH) groups, and the decomposition of trace mineral impurities naturally present in the beach sand. After fine milling (RA2), the intensity of these thermal events decreases, indicating improved particle homogeneity and a more uniform heat-transfer behaviour.

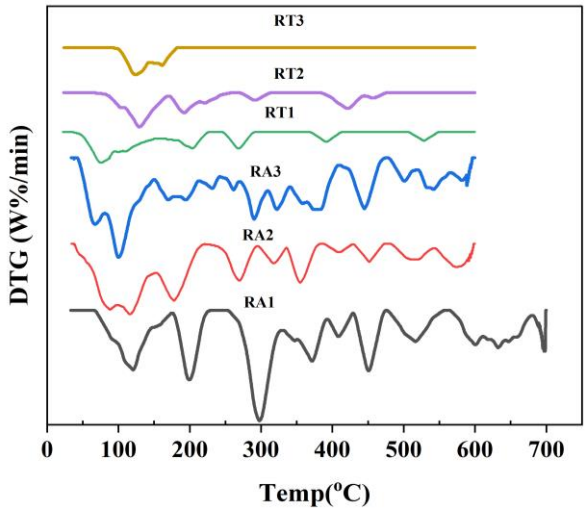


Fig.11: DTG curves of Adari silica sand before and after milling, acid treatment, and heat treatment.

Following acid treatment (RA3), the DTG curve becomes considerably smoother, with fewer and less intense thermal peaks. This behaviour confirms the effective removal of acid-soluble impurity phases, including iron oxides, alumina, carbonates, and

other accessory minerals, resulting in enhanced silica purity and thermal stability. Similar observations have been reported for purified quartz materials, where chemical treatment reduces the number of thermally active impurity phases and improves the thermal response of the material [25-30].

A remarkable improvement is observed after thermal treatment. The DTG curves of RT1, RT2, and RT3 are nearly flat, exhibiting only weak thermal events below approximately 200 °C, while almost no significant thermal reactions are detected at higher temperatures. The substantial reduction in both the number and intensity of DTG peaks demonstrates that calcination effectively removed residual hydroxyl groups and volatile species while preserving the crystalline quartz framework. Moreover, the nearly overlapping DTG curves indicate that increasing the calcination temperature from 1200 °C to 1600 °C produces only marginal changes in thermal behaviours, suggesting that structural stabilization is essentially achieved at 1200 °C. This observation is particularly important because it indicates that lower calcination temperatures may provide the required thermal performance while minimizing energy consumption during processing. The excellent agreement between the DTG results, the XRF analysis (showing high SiO_2 purity), and the XRD patterns (confirming the preservation of the crystalline quartz phase) demonstrates the effectiveness of the combined milling, acid purification, and heat-treatment processes. The resulting silica exhibits excellent thermal resistance, high chemical purity, and structural stability, making it a promising candidate for high-temperature welding consumables, where thermally stable silica enhances slag stability and weld quality. Furthermore, these characteristics are highly desirable for electronic and microelectronic devices, dielectric and insulating ceramics, and photovoltaic technologies, where high-purity silica with excellent thermal stability is required for glass substrates, insulating layers, and silicon-based functional materials. These findings are consistent with previous studies reporting that highly purified crystalline silica exhibits minimal thermal reactions because of its reduced impurity content, low hydroxyl concentration, and highly ordered crystal structure.

3.6. Results of Fourier Transform Infrared spectroscopy (FTIR) analysis:

Figure 12 presents the Fourier Transform Infrared (FTIR) spectra of silica sand from the Adri Al-Shati region at different processing stages, including the raw sand (RA1), finely milled sand (RA2), chemically treated sand (RA3), and the heat-treated samples (RT1–RT3). The spectra exhibit the characteristic absorption bands of crystalline silica (quartz), confirming that the principal chemical structure of the material was preserved throughout the purification and thermal treatment processes. The intense absorption band centred at approximately 1080 cm^{-1} is attributed to the asymmetric stretching vibration of the Si–O–Si network, while the band observed at approximately 460–480 cm^{-1} corresponds to the bending vibration of Si–O–Si bonds. These bands are characteristic of silica and are consistent with the FTIR features reported for quartz-rich silica materials [23].

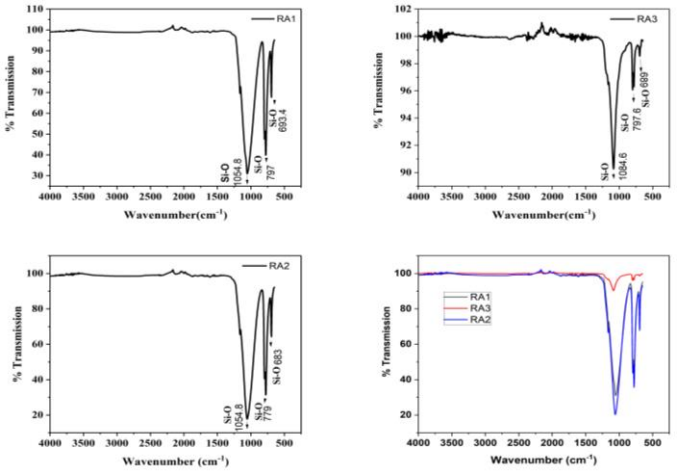


Fig.12: The peaks of the infrared spectrum of samples studied

Although all samples exhibited the characteristic silica absorption bands, slight variations in peak intensity were observed after milling, chemical purification, and heat treatment. Following acid treatment (RA3), the characteristic Si–O–Si bands became more distinct, indicating the effective removal of impurity phases that may partially mask the silica absorption bands. After heat treatment (RT1-RT3), the spectra remained essentially unchanged, while the Si– O –Si bending vibration near 460–480 cm^{-1} became slightly more prominent. This behavior suggests improved structural ordering of the quartz lattice after calcination rather than the formation of new chemical phases. No significant absorption bands were detected in the 1600- 4000 cm^{-1} region, where the stretching vibrations of hydroxyl (– OH) groups and physically adsorbed water are normally observed. The absence or very weak intensity of these bands indicates that the combined milling, chemical purification, and thermal treatment effectively reduced the amount of surface hydroxyl groups and adsorbed moisture, and supported the good structural stability of the SiO_2 phase under investigation.

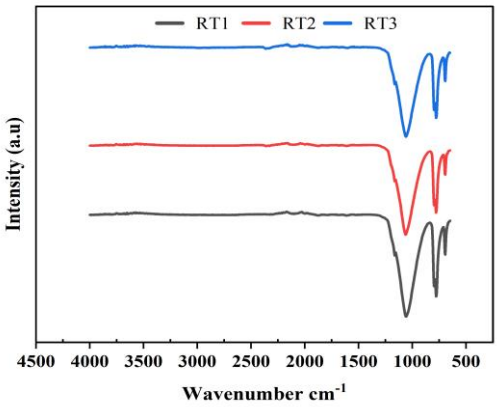


Fig.13: The peaks of infrared spectrum of RA3 after heat treatment RT1(1200 ^{O}C), RT2(1400 ^{O}C) and RT3 (1600 ^{O}C).

These observations are consistent with the TGA/DTG results, which showed minimal mass loss associated with moisture removal, and with the XRF analysis, which showed the increased SiO_2 purity after purification. Furthermore, the preservation of the characteristic quartz-related absorption bands is consistent with retention of the principal Si–O–Si bonding environment; the crystalline phase should be interpreted from XRD throughout the investigated processing stages. The combined FTIR, XRF, XRD, and thermal analyses demonstrate that the applied purification route successfully produced high-purity silica with good structural stability and favorable thermal characteristics. These properties provide a preliminary basis for further investigation of the prepared silica in welding-related applications, where the thermal and chemical stability of silica may contribute to flux and slag behavior. The purified silica may warrant further evaluation in electronic and photovoltaic-related applications, particularly with respect to chemical purity, hydroxyl content, and thermal stability [11,13,18].

Conclusion

This study successfully demonstrated the physicochemical viability of natural silica sand from Libya's Adri Al-Shati region as a high-purity industrial precursor. The key findings are summarized as follows:

- ✓ Mineralogical Integrity: XRD analysis confirmed that the raw sand maintains a stable hexagonal quartz structure.
- ✓ Effective Purification: The applied acid-leaching process achieved a significant increase in silica purity (SiO2), rising from 91.7% to 99.36%, while effectively reducing critical metallic

contaminants such as Fe2O3and CaO to electronic grade standards.

✓ Phase Evolution: Controlled thermal treatment established a predictable phase transformation pathway, where temperatures exceeding 1200°C induced significant transitions from α-quartz to tridymite and cristobalite, which are crucial for optimizing weld pool protection and slag rheology.

✓ Structural and Thermal Performance: The material demonstrated excellent thermal stability via TGA/DTG analysis, with refined crystallite sizes (~66 nm) and a well-defined particle size distribution (1.7–2.3 mm) ideal for industrial flux matrices.

In conclusion, the purified silica from the Adri region represents a valuable and sustainable local resource. By implementing this scalable chemical purification methodology, Libya can significantly reduce reliance on imported raw materials. The treated silica possesses the structural qualities and thermal consistency required to meet the stringent technical demands of the photovoltaic, electronic, and advanced metallurgical sectors, positioning it as a strategic asset for future industrial self-sufficiency

References

[1]- Zhang K, Yang T, Yang X (2023) Redox-independent low water solubility in quartz and implications for water storage in the crust. Journal of Geophysical Research: Solid Earth 128(4):e2022JB026189. https://doi.org/10.1029/2022JB026189

[2]- Pavan C, Escolano-Casado G, Bellomo C, Cananà S, Tomatis M, Leinardi R, Mino L, Turci F (2023) Nearly free silanols drive the interaction of crystalline silica polymorphs with membranes: implications for mineral toxicity. Frontiers in Chemistry 10:1092221. https:// doi.org/ 10.3389/ fchem.2022.1092221.

[3]- EIler RK (1979) The Chemistry of Silica: Solubility, Polymerization, Colloid and Surface Properties, and Biochemistry of Silica. Wiley, New York.

[4]- Sdiri A, Higashi T, Bouaziz S, Benzina M (2014) Synthesis and characterization of silica gel from siliceous sands of southern Tunisia. Arabian Journal of Chemistry 7:486–493. https://doi.org/10.1016 /j.arabjc.2010.11.007

[5]- Nekrashevich SS, Gritsenko VA (2014) Electronic structure of silicon dioxide: a review. Physics of the Solid State 56:207–222. https:// doi.org/ 10.1134/S106378341402022X

[6]- Xakalashe BS, Tangstad M (2011) Silicon processing: from quartz to crystalline silicon solar cells. In: Jones RT, den Hoed P (eds) Southern African Pyrometallurgy 2011. Southern African Institute of Mining and Metallurgy, Johannesburg, pp 83–100.

[7]- Heaney PJ, Prewitt CT, Gibbs GV (eds) (1994) Silica: Physical Behavior, Geochemistry and Materials Applications. Reviews in Mineralogy, vol 29. Mineralogical Society of America, Washington, DC.

[8]- Kou S (2021) Welding Metallurgy, 3rd edn. John Wiley & Sons, Hoboken, NJ.

[9]- Mills KC (2011) The Estimation of Slag Properties. Course notes, Pyrometallurgy 2011 Conference, Misty Hills, South Africa.

[10]-Grimm H, Dorner B (1975) On the mechanism of the α–β phase transformation of quartz. Journal of Physics and Chemistry of Solids 36:407–413.

[11]-Qamati H, Rahmanifard R, Jafari F, Savabieh HR (2025) Mechanical and thermal properties of fused silica ceramic composites with Cr_2O_3 and Al_2O_3 additives. Ceramics International 51:24032–24042. https://doi.org/10.1016/j.ceramint.2025.03.088

[12]-Kingery WD, Bowen HK, Uhlmann DR (1976) Introduction to Ceramics, 2nd edn. Wiley, New York.

[13]-Jennings A, Senior A, Guerin K, et al. (2024) A review of high-purity quartz for silicon production in Australia. Australian Journal of Earth Sciences 71:1085–1097. https:// doi.org/ 10.1080/ 08120099 .2024. 2362296

[14]-Bulatovic SM (2015) Beneficiation of silica sand. In: Handbook of Flotation Reagents: Chemistry, Theory and Practice. Elsevier, pp. 121–127.

[15]-Conte R, Izquierdo DR, Francesco G (2023) Submerged arc welding process: a numerical investigation of temperatures, displacements, and residual stresses in ASTM A516-Gr70 corner joined samples. International Journal of Advanced Manufacturing Technology 127:5437–5448. https://doi.org/10.1007/s00170-023-11908-x

[16]-El-Hawat AS, El-Ghali MAK, McLaren SJ, Kemp SJ (2021) Early silicification of the Cyrenaican chert, Libya: the importance of moganite as a transitional silicon dioxide phase. Sedimentology 68:855–880. https://doi.org/10.1111/sed.12809

[17]-Ramakrishna Reddy S, Pandey NK, Mondal S, Sivaraman N (2020) Catalytic reduction of U(VI) with hydrazine using Pt/SiO_2 catalyst in nitric acid medium—kinetics and equilibrium. Journal of Radioanalytical and Nuclear Chemistry 325:425–434. https:// doi.org/ 10.1007/ s10967-020-07265-8

[18]-Goudarzi GH (1970) Geology and Mineral Resources of Libya—A Reconnaissance. US Geological Survey Professional Paper 660. US Government Printing Office, Washington, DC, 104 pp. https://doi.org/10.3133/pp660

[19]-Zreiba NA, Dweiby RM (2014) Libyan quartz as candidate for solar grade silicon production. 2014 5th International Renewable Energy Congress (IREC). IEEE. https://doi.org/10.1109/IREC. 2014.6827035.

[20]-Boussaa S, Zaourar Boutarek N, Kefaifi A (2020) Characterization and experimental design application for Algerian silica sand enrichment. Arabian Journal of Geosciences 13:472. https:// doi.or g/ 10.1007/ s12517-020-05489-2

[21]-Bakri S, Anas M, Wakila MH, Chalik CA (2023) Geochemical characterization of silica sand in the Sidenreng Rappang area based on X-ray diffraction analysis and X-ray fluorescence analysis. Journal of Geology and Exploration 2:1–7. https://doi.org/10.58227/jge.v2i1.36

[22]-Jenkins R (1999) X-Ray Fluorescence Spectrometry. Wiley, New York.

[23]-Ellerbrock R, Stein M, Schaller J (2022) Comparing amorphous silica, short-range-ordered silicates and silicic acid species by FTIR. Scientific Reports 12:11708. https://doi.org/10.1038/s41598-022-15882-4

[24]-MacKenzie KJD, Smith ME (2002) Multinuclear Solid-State Nuclear Magnetic Resonance of Inorganic Materials. Pergamon, Oxford.

[25]-Ibrahim AFM, Seifelnassr AAS, Al-Abady A, et al. (2022) Characterization and iron removal enhancement of El-Zaafarana white sand. Mining, Metallurgy & Exploration 39:2187–2198.https:// doi.org/10.1007/s42461-022-00667-0

[26]-Ramadan FS, El-Shafei SA, Henaish AA, Essawy MA (2023) Evaluation of white sand deposits for industrial applications: a case study from Abu Zenima area, Sinai, Egypt. Bulletin of the Faculty of Science, Zagazig University2023(2):42–57. https:// doi.org/ 10.21608/ bfszu.2023.173732.1203

[27]-Patterson AL (1939) The Scherrer formula for X-ray particle size determination. Physical Review 56:978–982. https:// doi.org/ 10.1103/ PhysRev.56.978

[28]-Gaber MAW, Hamed TE, Selim YA, Lotfy NM (2024) Upgrading of silica sand using chemical leaching process for industrial application at Wadi El Dakhal area, Egypt. Egyptian Journal of Petroleum 33(4): Article 7. https://doi.org/10.62593/2090-2468.1054

[29]-Kono MC, Batu MS, Kedang YI, Seran R (2021) XRF and XRD investigation for the results of the extraction of mud volcano from Napan village into silica. JKPK (Jurnal Kimia dan Pendidikan Kimia) 6(3):317–325. https://doi.org/10.20961/jkpk.v6i3.55022